Quench Protection of Nb_3Sn High Field Magnets Using Heaters, a Strategy Applied to the Graded Racetrack Dipole R2D2

T. Salmi, D. Liu, V. Calvelli, and E. Rochepault

***Abstract*—The quench protection for the Future Circular Collider (FCC) 16 T Nb_3Sn dipoles was based either on the CLIQ (Coupling Loss Induced Quench) system, or on resistive quench protection heaters. Several heater designs were sketched during the iterative magnet design processes. This led to identifying some rules about an effective heater design in the full-scale 14-m-long magnets. Following the FCC study, short dipole magnet models are being built to test the novel features that were envisioned for the FCC magnets. In this work, we review the principles of effective heater design, and then apply this methodology to the graded block dipole short model R2D2, which is being designed at CEA Saclay. This magnet has high current density in copper after quench, which makes the protection challenging and requires pushing the heater technology to its limits.**

***Index Terms*—Accelerator magnets, protection heaters, Nb_3Sn dipoles quench protection.**

I. Introduction

DIPOLE magnets with high magnetic field are being developed to enable future particle accelerators with higher energy particle beams and consequently higher collision energies [1], [2]. The accelerator dipoles in the CERN LHC and in the conceptual design of Future Circular Collider (FCC) are 14 m long. In the technology development process several short model magnets are always built to test novel technologies and behavior of the conductor and magnet structure in higher fields. An important part of magnet design is their quench protection, meaning the safety system ensuring that the conductor will not overheat in case of a sudden transition from superconducting to normal conducting state. Especially for long high-field high-energy density magnets, the quench protection should be integrated into the early magnet design.

In an accelerator, several dipole magnets are powered in series. In case a quench is detected, the quenched magnet is decoupled from the rest of the circuit and protective heating system is activated in the magnet. The purpose of the heating is to bring the coils uniformly to resistive state and drive a fast decay of the operation current. The existing accelerators (Tevatron and LHC) use resistive quench protection heaters, but in the HL-LHC a new system based on CLIQ (Coupling Loss Induced Quench) will be used together with the heaters [3]. The individual short model magnets (approximately 1 m long) often can be protected with external dump resistor in laboratory tests.

In this paper we first review the main steps in the heater design process based on the experience from the FCC 16 T Nb_3Sn dipoles conceptual design [4]. We then apply the principles to the R2D2 short model, that is being designed at CEA to study the intra-layer grading that was foreseen for the FCC 16 T block-type dipole and the impact of very high current density to protection [5]. The first goal is to summarize the heater design strategy in a way that it can be applied also in other future accelerator magnet design processes. The second goal is to evaluate the feasibility of only quench heaters-based protection in the R2D2, and outline directions for future protection design studies. In parallel, an analysis of the feasibility of only CLIQ -based protection was carried out [6]. The combination of heater and CLIQ will be carried out at a later stage. In the coming tests, the R2D2 protection can be ensured with a dump resistor, and this makes it a useful test bed for evaluating the efficiency of different protection technologies that will be vital for longer magnets.

II. Principles of Heater Design Process

A. Heater Technology

The heaters in accelerator magnets are typically based on stainless steel strips (25 μm thick) on coil surfaces. They are insulated from the coil by polyimide (25–75 μm thick) and sometimes an additional layer of fiber glass [7], [8]. Periodical copper cladding (5–10 μm thick) on the stainless steel is used to reduce the strip overall resistance and allow focusing the heating into the so-called heating stations (HS). Cable quenches under the HS and the longitudinal quench propagation will bring the segment between HS to resistive state. The strips are typically U-shaped, extending the entire coil length and back. The strips are connected in circuits that are powered with a capacitor bank discharge upon the protection activation. The heater peak power, P_0, is expressed as the dissipated power divided by area facing

Manuscript received 13 November 2022; revised 6 February 2023; accepted 11 February 2023. Date of publication 8 March 2023; date of current version 16 March 2023. This work was supported by Academy of Finland HiQuench-Project under Grants 334318 and 336287. *(Corresponding author: Tiina Salmi.)*

T. Salmi is with Tampere University, 33720 Tampere, Finland (e-mail: tiina.salmi@tuni.fi).

D. Liu was with Tampere University, 33720 Tampere, Finland. He is now with the LUT University, 15210 Lahti, Finland.

V. Calvelli and E. Rochepault are with IRFU, CEA, Université Paris-Saclay, F-91191 Paris, France.

Color versions of one or more figures in this article are available at https://doi.org/10.1109/TASC.2023.3251280.

Digital Object Identifier 10.1109/TASC.2023.3251280

the heated coil. It can be computed based on heater current density (J_{ss}), stainless steel resistivity (ρ_{ss}) and heater thickness (d_{ss}) using $P_0 = J_{ss}(t = 0)^2 \rho_{ss} d_{ss}$. The heater current decays according to the time constant, τ_{RC}, which is the product of circuit capacitance and total resistance. More information on the technology and used terminology can be found from [9].

B. Steps in the Heater Design Process

The goal is to design the heater strips to bring a sufficiently large fraction of coil volume to resistive state in a time short enough. The proposed design process includes five steps:

Step 1. Estimation of the required response time of the quench protection system: This requires setting the maximum allowed hotspot temperature. The analysis can then be done using the time margin concept [10], the energy margin method [11], or via simulations of a uniform quench and the following current decay in the coil using for example Coodi [12] or ROXIE [13]. The computation has to take into account the Joule heating in the original quench location during the detection and protection system delay times (assume constant current) and during the subsequent current decay. The result of this analysis is the required "protection delay time" or "time margin" which includes the detection time, validation time, switches delays and the average heater delay time.

If possible, one should also estimate the quench detection time at this stage. The estimation may be based on the coil resistive voltage development (in the most critical turn), and the needed delay for the electronics. This allows estimating the maximum delay for the protection system to quench the coil.

Step 2. Computation of feasible heater delays and mapping the parametric dependence of heater delay: This requires setting the key heater technology limitations (insulation thickness, strip thickness, Cu-plating thickness). The calculation can be done by modeling the heat conduction from the heater to the cable in 2D (longitudinally along the cable) and computing how long it takes to exceed the current sharing temperature. Tools to do this are for example CoHDA [14], or COMSOL [8]. The prediction power in this simulation approach is typically quite good at high current, but decreases at low currents, or at lower field region [15], [16].

One can first simulate the delays with very high heater power (highest possible not to overheat the strip itself) to get the reference possible minimum delay. Then one can do a parametric study with different heater peak power, heater voltage decay time constant, and heating station length. The analysis should include the different cables, field regions and different operation conditions. The delays obtained for average field in the coil blocks can be compared with the needed average delay estimated in Step 1, and one already gets an idea of the feasibility of heater based protection.

Step 3. Analysis of the coil internal voltages and resistance development characteristics: This step can be done by simulating a uniform quench in the coil (e.g., using Coodi, ROXIE, or COMSOL-based models [17]) and looking at potential to ground along the coil turns. The inductive voltage typically has a larger component in the low-field region. One may need to consider this in the heater design so that these turns are quenched relatively quickly to increase their resistance and balance the inductive voltage [12]. If the coil is graded, e.g., uses different cable in high field (HF) and low field (LF) region, the cables may participate differently. In particular, the resistance may grow faster in the smaller LF cable. In long magnets, these features may imply a heater design that focuses more heat on LF region/cable. In contrary, in small single-cable magnets where the voltages are not a problem, it is more efficient to heat the high field region first [18].

Step 4. Design strip geometries and heater powering circuits: This requires setting the charging voltage, capacitance and number of capacitor banks used for heater powering. The strip geometries (width, length of heating station, distance between heating stations) must be designed considering the total available heater powering energy. One approach is to start by defining the ideal HS length and power for different field regions, based on the results from steps 2 and 3. After this, one decides the type of heater geometry (for example a straight strip or a stair-case type shape). After this one can compute the obtainable heater powers assuming different circuit powering configurations (number of strips in parallel or in series) and different distance between HS and strip widths (total resistance of each strip). It is important to add some margin (0.5–1.0 Ω) to the strip resistance for wires, etc. An Excel table can be helpful in computing the powers.

Step 5. Simulation of magnet current decay and the resulting hotspot temperature and voltages: After finding an attractive heater geometry in step 4, one has to simulate the magnet current decay based on the induced resistance increase in coil. One way to do this is to first simulate the delays in different coil regions, and then compute the current decay with Coodi, which takes the simulated heater delays and quench propagation velocities as input. This approach gave reasonable results when compared to HL-LHC magnet tests [16]. If the HS is long enough so that it can be simulated as 1D heat conduction from heater to cable, then more tools are available. If a dump resistor or CLIQ is used together with the heaters, its impact should be considered within this and the previous step.

III. Case Study: Heater Design for R2D2

A. Magnet Parameters and Heater Design Constraints

The R2D2 magnet geometry is shown in Fig. 1, and its parameters are summarized in Table I. In this analysis we assume 50 μm polyimide insulation from heater to coil, which is 25 μm less than in long FCC magnets due to lower voltages. We consider powering the heaters with two capacitor banks, each with 450 V and 19.2 mF. The capacitor bank values may be updated later based on the test facility equipment.

We assume that the longitudinal quench propagation velocity between heating stations is 20 m/s, and that there is 10 ms turn-to-turn quench propagation time from the neighboring turns for the coil turns that are not covered by a heater.

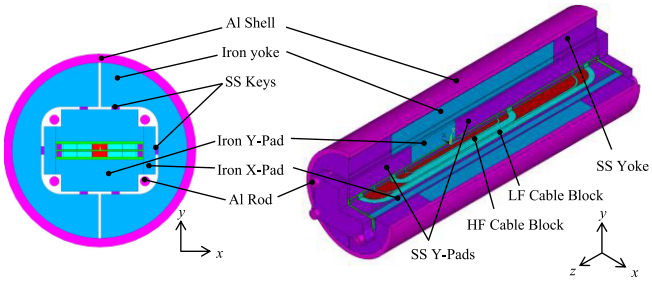

Fig. 1. Left: Cross-section of the R2D2 coils and the mechanical components around them. Right: 3D schematics showing the high field- and low field cable blocks [21].

TABLE I
MAGNET PARAMETERS USED IN HEATER DESIGN

Magnet	R2D2, v.8.14.R2	
I_{nom} at 4.2 K (A)	14588	
B_{peak} at I_{nom}, 4.2 K (T)	12.37	
L_d at I_{nom} (mH/m)	4	
Magnetic equivalent length (m)	0.835	
Cable	HF	LF
Number of turns	16	21
Cable width x thickn. (bare) (mm^2)	12.74 x 2.06	12.73 x 1.31
Number of strands	21	34
Strand diameter (mm)	1.1	0.7
Cu/SC	0.9	1.8
RRR	200	450
Strand twist pitch (mm)	84	93
Cable insulation thickn,, G10 (mm)	0.15	0.15
c0 for Jc fit at 4.2 K (A^2 /mm^2) [19]	230984	195500

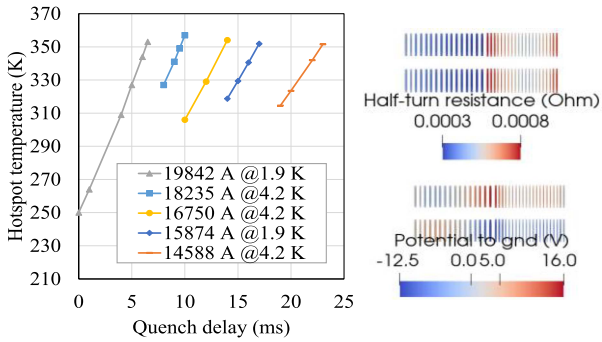

Fig. 2. Left: Hotspot temperature vs protection delay in R2D2. Right: Distribution of resistances and voltages to ground in the turns of the half-coils cross-section after uniform quench.

B. Step 1: Analysis of Needed Heater Delays

The first step in the analysis was to simulate the coils temperature evolution after inducing a uniform and instantaneous quench in all coil turns. The hotspot temperature is computed adiabatically based on the Joule heat by the magnet current during the quench delay and the subsequent current decay. The simulation was done with Coodi. The hotspot temperature vs. the uniform quench delay is shown inFig. 2.

The delay time related to the maximum allowed temperature, 350 K, is 23 ms at nominal current, I_{nom}, at 4.2 K (14588 A). It decreases to 6 ms at short sample current at 1.9 K (19842 A). These times are very short compared to the FCC study which

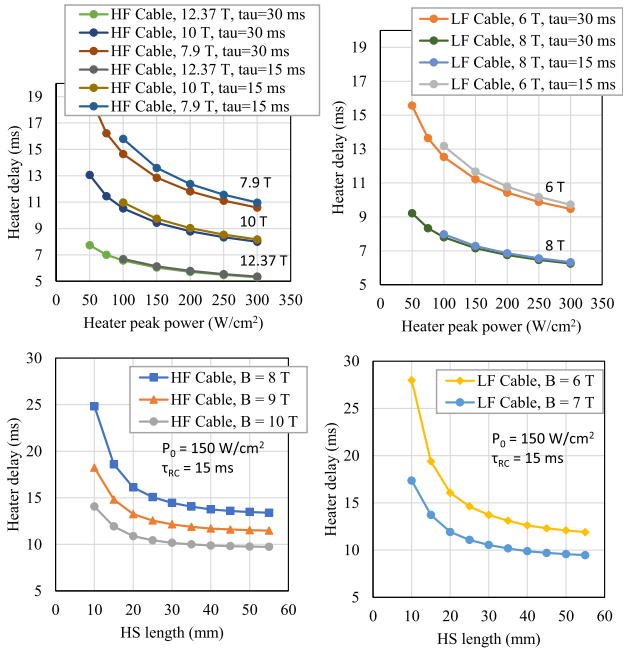

Fig. 3. Heater delay as a function of heater power or heating station length.

allocated ~20 ms for only detection and validation. The highest hotspot temperature occurs in case of a quench is in the LF cable with the highest field.

The RRR of LF cable is expected to be unusually high (450) [20]. To quantify the impact of LF cable RRR on the hotspot temperature, the simulation for the nominal current case at 4.2 K with 23 ms delay time was repeated with RRR values of 200 and 100. The results suggests that the hotspot temperature increases by less than 3 K, even if the RRR decreased down to 100. The stronger heating at constant current was compensated by a faster current decay.

C. Step 2: Computation of Obtainable Heater Delays

Heater delay is simulated in HF and LF cable using CoHDA. The delay vs. heater peak power is shown in Fig. 3. There is no saturation, and the delay decreases as the peak power is increased. It also shows the impact of the circuit *RC*-time constant (τ_{RC}). Above 150 W/cm^2, a time constant smaller than of 15 ms starts to increase the delay. The results are shown for the maximum and minimum magnetic field in the HF and LF cable blocks. For the same field value, the LF cable would quench faster, because its superconductor current density is over two times higher than in the HF cable, so its critical temperature is lower.

The impact of heating station length is shown in Fig. 3. In general, one would like to have a sufficiently long HS not to increase the delay, but not too long because shorter length allows more HS and more propagating fronts. It seems that about 20 mm is needed in high field regions and 40 mm in low field regions.

Average delay of 8–10 ms is possible at nominal current if high heater power is used (200–300 W/cm^2). Compared with the needed protection delay based on step 1, the feasibility of

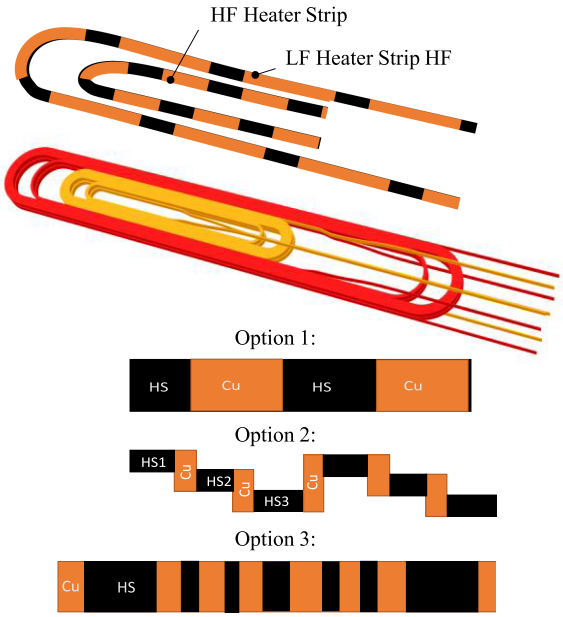

Fig. 4. From top to bottom: A schematic of the U-shaped heater strips on the coil surfaces, 3D view of the LF (red) and HF (orange) coils, and the three heater layout options. Option 1 is a regular straight strip, option 2 is a staircase with variable length heating stations, and option 3 is a straight strip with variable length heating stations. The strips repeat this pattern to make a U-shape that extends the entire coil length and back. The orange represents copper and black stainless steel heating stations.

only heater-based protection seems very challenging: The time available to detect the quench and quench the coils was 23 ms. If we were able to use the very high heater power in all coils, and obtain 8–10 ms average heater delays, only 13–15 ms is left for the detection. Even if this was possible, there is very little room for redundancy to cope with failure cases. We however complete the study to see the potential efficiency of practical heaters.

D. Step 3: Guidance for Heater Delay Distribution Based on Voltages and Resistance Development

We used Coodi simulations to analyze the resistance distribution in the coil after a uniform quench. The simulation takes into account the difference in HF and LF cables Cu areas, magnetic fields, RRR's, and temperature evolutions due to the losses. The resistance in the coil LF block turns is higher than in the HF block turns, see Fig. 2. The turns with the highest resistance are the LF cables with the highest field.

The voltages in this short magnet are only a few tens of volts. Therefore, the heater design can focus on reducing the hotspot temperature. In this pursuit, it is more efficient to aim to quench first the LF turns with high field.

E. Step 4: Heater Geometries and Heater Circuits

In this first iteration of the heater design, we consider one strip per HF block and one for LF block. The strips follow the coil blocks in the return end to make a U-shape, as shown in Fig. 4. The length of the HF strip is 1.2 m and that of LF is 2.7 m. The HF strips of both coils are connected in parallel to one capacitor, and the LF strips to one. We assume 0.5 Ω margin in series with each heater circuit. This configuration is not optimal because the longer strips dilute the heating energy in the LF block, which was the main driver for coil resistance development. The reason for this design decision was to allow testing LF and HF strips separately. The future design iterations will consider also other options, and adding more capacitor banks. Three different heater geometry options are considered, as sketched in Fig. 4.

1) Option 1: A Regular Straight: A regular straight strip has periodic stainless steel heating stations and copper between them. The strip widths are 30 mm, covering 80% of the HF block width and 88% of the LF block width. This width was chosen to cover as many turns as possible while keeping the peak power and time constant still high enough (above 200 W/cm^2 and not much below 15 ms). The HS lengths are based on the lowest field under heater and are 4 cm in HF and 4.5 cm in LF. Copper segment lengths between HS were decided 5 cm and 12 cm leading to $P_0 = 240$ W/cm^2, $\tau_{\mathrm{RC}} = 13$ ms in HF heater and $P_0 = 200$ W/cm^2 and $\tau_{\mathrm{RC}} = 14$ ms in LF.

2) Option 2: A Tunable Staircase: In the staircase geometry the heating station length (or width) can be varied based on the field region under it. In this design the heater strip for HF block has three heating stations per period, each 11.5 mm wide and the LF heater has two, each 16 mm wide. The heater covers 91% of HF block and 94% of LF block turns. The lengths of the heating stations are in HF heater: 25 mm, 30 mm, and 40 mm, period being 12 cm. The resulting powers are $P_0 = 300$ W/cm^2, $\tau_{\mathrm{RC}} = 25$ ms. In LF heater the heating station length are 35 mm and 40 mm, and period is 17 cm. This results to $P_0 = 250$ W/cm^2 and τ_{RC} 22–26 ms. This option can cover more turns while still obtaining high power. The downside is that there is a minimum length for the period based on the total length of the heating stations.

3) Option 3: A Novel Distributed HS: This is a straight heater with variable heating station length: shorter heating stations are placed between longer ones. At high current also the shorter HS may quench the cable, but if not, they will pre-heat the cable for faster quench propagation between the longer HS. At low current the longest HS quench a sufficient fraction of the coil. In the example heater we have 4 cm for the longest HS and 1 cm for the shortest HS.

This type of heater option would be particularly interesting for long magnets, where the impact of quench propagation between HS is larger. For example, the distance between HS in the FCC magnets was up to 30 cm, corresponding to 7.5 ms propagation time with 20 m/s [4]. Inducing an additional hotspot in the middle of the period at high current could double the resistance development rate and half the propagation time.

This type of heater would be also interesting when used in combination with CLIQ. It enhances the potential of the heaters to deposit wanted energies locally into the coil. CLIQ distributes its capacitor bank energy more evenly into the coils, which leads to a widespread quench at high current, but at lower currents it would be more efficient, and sufficient, to focus the energy more

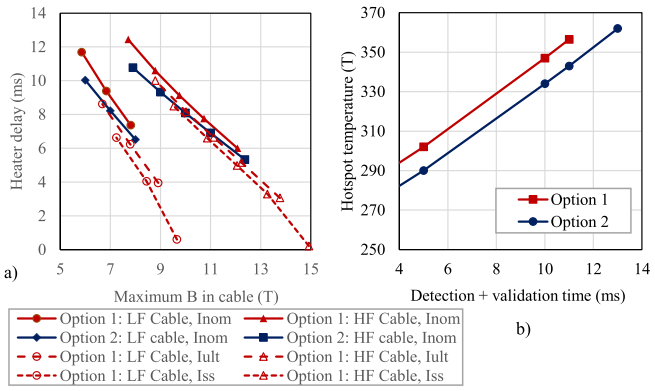

Fig. 5. (a) Heater delay as a function of cable magnetic field for heater options 1 and 2 at nominal current (Inom), ultimate current (Iult) and shortsample current (Iss) at 4.2 K. (b) Simulated hotspot temperature at nominal current as a function of time delay before heater activation.

locally in order to limit the total energy. Combining the more uniform heating by CLIQ with specifically targeted heated spots by heaters could be designed to cover all magnet operation points in an optimal way.

To properly consider this heater design option, one needs to compute the impact of heat diffusion from quench propagation. This was not done for this paper, but it will be the future work.

F. Step 5: Simulated Hotspot Temperatures

The heater delays with the above-described heater options 1 and 2 were simulated at different field regions and summarized in Fig. 5(a). The delays are shown vs. the maximum magnetic field in the cables. In a coil, the delay in each turn would be defined by the magnetic field in it, and whether it is covered by a heater or not. The first quench after heater activation at nominal current at 4.2 K is 7.5 ms for option 1, and 6.6 ms for option 2. The average delay was 12.4 ms for option 1 and 10 ms for option 2. This is without the quench propagation between HS, but accounting for transversal quench propagation to the turns that are not covered by a heater. When including propagation between HS assuming 20 m/s, the average delay to quench all turns totally is 14.4 ms with option 1, and 13 ms with option 2.

Fig. 5(b) shows the simulated hotspot temperature as a function of time between original quench and heater activation for heater options 1 and 2 at nominal current at 4.2 K. It shows that detection time of 10 ms is required for option 1 to stay below 350 K, and 11.5 ms if using option 2. In the case of detection time 10 ms, the designed practical heaters give approximately 20 K higher temperature than if all the coils were covered with the heater. Covering all the coils with heater would require at least 5 HFU's instead of 2. This suggests that only minor improvements can be done with further iterations of the heater geometry.

The analysis at higher currents at 4.2 K was performed for option 1. To stay below 350 K at ultimate current, the detection time should be 4 ms, and at short sample current it should be less than 2 ms, which is not achievable with today's technology.

IV. Discussion and Conclusion

The outlined heater design process was applied to a short model magnet with particularly stringent protection requirements. Following the process we were able to quickly estimate the feasibility of heater based protection, and sketch the first heater designs. In this short magnet the average heater delay plus the quench propagation between heating stations was about 13-14 ms at nominal current. In the simulations quench detection time within 10 ms was required in order to keep peak temperature below 350 K. This fast detection time is difficult to achieve in the real magnet. It seems thus that heaters alone cannot guarantee a reliable protection in R2D2.

Since R2D2 short magnet can be protected with a dump resistor, it could provide a test bench for future iterations of new heater designs given that they will demonstrate a significant gain with respect to the state-of-the-art heater technology for long magnets. The dump resistor activation after measuring the heater-induced start of the magnet resistance increase will ensure magnet safety while still providing valuable data about heater efficiency.

References

[1] A. Abada et al., "FCC-HH: The hadron collider," *Eur. Phys. J. Special Topics*, vol. 228, pp. 755–1107, 2019, [Online]. Available: https://doi.org/10.1140/epjst/e2019-900087-0

[2] A. Abada et al., "HE-LHC: The high-energy large hadron collider," *Eur. Phys. J. Special Topics*, vol. 228, pp. 1109–1382, 2019, [Online]. Available: https://doi.org/10.1140/epjst/e2019-900088-6

[3] E. Ravaioli et al., "Quench protection studies for the high luminosity LHC Nb3Sn quadrupole magnets," *IEEE Trans. Appl. Supercond.*, vol. 31, no. 5, Aug. 2021, Art. no. 4700405, doi: 10.1109/TASC.2021.3055160.

[4] T. Salmi, M. Prioli, A. Stenvall, and A. P. Verweij, "Quench protection of the 16 T Nb3Sn dipole magnets designed for the future circular collider," *IEEE Trans. Appl. Supercond.*, vol. 29, no. 5, Aug. 2019, Art. no. 4700905, doi: 10.1109/TASC.2019.2895421.

[5] V. Calvelli et al., "R2D2, the CEA graded Nb3Sn research racetrack dipole demonstrator magnet," *IEEE Trans. Appl. Supercond.*, vol. 31, no. 5, Aug. 2021, Art. no. 4002706, doi: 10.1109/TASC.2021.3075298.

[6] D. Liu, T. Salmi, V. Calvelli, and E. Rochepault, "CLIQ protection design for the graded Nb_3Sn research racetrack dipole demonstrator (R2D2)," *IEEE Trans. Appl. Supercond.*, doi: 10.1109/TASC.2023.3247983.

[7] M. Baldini et al., "Assessment of MQXF quench heater insulation strength and test of modified design," *IEEE Trans. Appl. Supercond.*, vol. 31, no. 5, Aug. 2021, Art. no. 4701305, doi: 10.1109/TASC.2021.3058223.

[8] S. I. Bermudez et al., "Quench protection studies of the 11-T Nb3Sn dipole for the LHC upgrade," *IEEE Trans. Appl. Supercond.*, vol. 26, no. 4, Jun. 2016, Art. no. 4701605, doi: 10.1109/TASC.2016.2536653.

[9] H. Felice et al., "Instrumentation and quench protection for LARP Nb3Sn magnets," *IEEE Trans. Appl. Supercond.*, vol. 19, no. 3, pp. 2458–2462, Jun. 2009, doi: 10.1109/TASC.2009.2019062.

[10] E. Todesco, "Quench limits in the next generation of magnets," in *Proc. WAMSDO, CERN Yellow Report CERN-2013-006*, 2013, pp. 10–16. [Online]. Available: https://doi.org/10.5170/CERN-2013-006.10

[11] T. Salmi and D. Schoerling, "Energy density method: An approach for a quick estimation of quench temperatures in high-field accelerator magnets," *IEEE Trans. Appl. Supercond.*, vol. 29, no. 4, Jun. 2019, Art. no. 4900116, doi: 10.1109/TASC.2018.2880340.

[12] T. Salmi et al., "Quench protection analysis integrated in the design of dipoles for the future circular collider," *Phys. Rev. Accelerators Beams*, vol. 20, no. 3, 2017, Art. no. 032401, doi: 10.1103/PhysRevAccelBeams.20.032401.

[13] S. Russenschuck, "ROXIE: A computer code for the integrated design of accelerator magnets," in *Proc. 6th Eur. Part. Accel. Conf.*, 1999, pp. 2017–2019.

[14] T. Salmi et al., "A novel computer code for modeling quench protection heaters in high-field Nb_3Sn accelerator magnets," *IEEE Trans. Appl. Supercond.*, vol. 24, no. 4, Aug. 2014, Art. no. 4701810, doi: 10.1109/TASC.2014.2311402.

[15] T. Salmi, G. Chlachidze, M. Marchevsky, H. Bajas, H. Felice, and A. Stenvall, "Analysis of uncertainties in protection heater delay time measurements and simulations in Nb3Sn high-field accelerator magnets," *IEEE Trans. Appl. Supercond.*, vol. 25, no. 4, Aug. 2015, Art. no. 4004212, doi: 10.1109/TASC.2015.2437332.

[16] T. Salmi, T. Tarhasaari, and S. Izquierdo-Bermudez, "A database for storing magnet parameters and analysis of quench test results in HL-LHC Nb3Sn short model magnets," *IEEE Trans. Appl. Supercond.*, vol. 30, no. 4, pp. 1–5, Jun. 2020, Art. no. 4703705, doi: 10.1109/TASC.2020.2981304.

[17] L. Bortot et al., "A consistent simulation of electrothermal transients in accelerator circuits," *IEEE Trans. Appl. Supercond.*, vol. 27, no. 4, Jun. 2017, Art. no. 4001305, doi: 10.1109/TASC.2016.2639585.

[18] T. Salmi and A. Stenvall, "The impact of protection heater delays distribution on the hotspot temperature in a high-field accelerator magnet," *IEEE Trans. Appl. Supercond.*, vol. 26, no. 4, Jun. 2016, Art. no. 4001405, doi: 10.1109/TASC.2016.2517238.

[19] EuroCirCol WP5 members, "16 T dipole design options: Input parameters and evaluation criteria," *CERN*, Geneva, Switzerland, Tech. Rep., 2015. [Online]. Available: https://indico.cern.ch/event/441684/

[20] S. Hopkins, "Status of conductor procurement," in *Proc. FCC Magnets Collaboration Meeting*, Dec. 10, 2019. [Online]. Available: https://indico.cern.ch/event/860937/contributions/3668944/

[21] E. Rochepault et al., "3D conceptual design of R2D2, the research racetrack dipole demonstrator," *IEEE Trans. Appl. Supercond.*, vol. 32, no. 6, pp. 1–5, Sep. 2022, Art. no. 4004605, doi: 10.1109/TASC.2022.3158634.